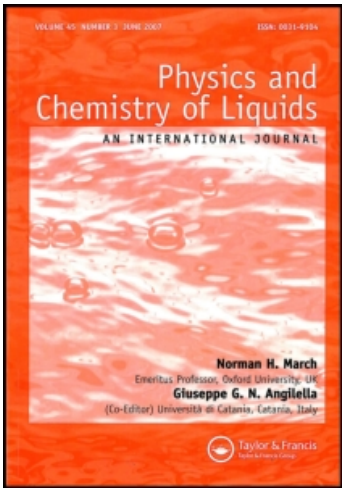

Physics and Chemistry of Liquids
Publication details, including instructions for authors and subscription information:
http://www.informaworld.com/smpp/title~content=t713646857

Structural Quantum Effects in Hydrogeneous Liquids and Glasses Part II Experiments using Synchrotron Radiation

P. A. Egelstaff[a]
[a] Department of Physics, University of Guelph, Guelph, Ontario, Canada

Online publication date: 27 October 2010

To cite this Article Egelstaff, P. A.(2003) 'Structural Quantum Effects in Hydrogeneous Liquids and Glasses Part II Experiments using Synchrotron Radiation', Physics and Chemistry of Liquids, 41: 2, 109 — 121
To link to this Article: DOI: 10.1080/0031910021000061042
URL: http://dx.doi.org/10.1080/0031910021000061042

Physics and Chemistry of Liquids
2003, Vol. 14, No. (2), pp. 109–121

Taylor & Francis
Taylor & Francis Group

Review

STRUCTURAL QUANTUM EFFECTS IN HYDROGENEOUS LIQUIDS AND GLASSES PART II EXPERIMENTS USING SYNCHROTRON RADIATION

P.A. EGELSTAFF

Department of Physics, University of Guelph, Guelph, Ontario, Canada

(Received 20 September 2002)

In Part I, the basic features of radiation scattering experiments and their application to hydrogeneous liquids and glasses were discussed. Initial experiments which explored the structural differences between hydrogenated and deuterated liquids or glasses were reviewed. In Part II, the advantages of using modern synchrotron radiation sources, especially their use to obtain higher quality data more rapidly, will be described. Then the recent results on water, benzene, amorphous ice, methanol and ethanol (obtained by these methods) will be discussed. It is concluded that this field has developed to the point where very interesting experiments (from both the observational and theoretical points of view) may be conducted reasonably quickly and with good precision. Moreover the programs reviewed here have produced results which have been of value both in testing modern theories for liquids and glasses, and in contributing to the improvement of the experimental methods used in these fields.

Keywords: Hydrogeneous materials; Quantum effects; Synchrotron radiation

1. INTRODUCTION

The initial series of experiments (described in Part I) showed that quantum effects related to molecular liquid structures were measurable using short wavelength E.M. radiation. The experiments reviewed in Part I used a 0.208 Å γ-ray source, and the short wavelength led to a reduction in the size of experimental errors and corrections compared to conventional X-ray methods for the measurement of the liquid structure factor. This approach had been suggested by Egelstaff in the early 80's [1]. Such experiments showed first that structural quantum effects in liquids were measurable, and secondly they provided data to compare to current theoretical predictions. Also the differences observed between the H and D isotopic samples (e.g. H_2O and D_2O) provided information to interpret more fully the experimental data on partial structure factors obtained by conventional neutron scattering techniques. And finally they paved the way towards more detailed and significant experiments when more intense high

ISSN 0306-7319 print: ISSN 1029-0451 online © 2003 Taylor & Francis Ltd
DOI: 10.1080/0031910021000061042

energy radiation sources became available. During the past six years intense beams of synchrotron radiation, with energies about 100 keV, have been used to improve and extend the fields of research which were described in Part I. These new methods and results will be reviewed here.

Consequently (for this field) the improvements in the ranges and quality of the data offered by intense synchrotron sources were most appropriate. Perhaps the most obvious improvement over the radioactive sources was in photon fluxes, which have allowed thinner samples to be used with smaller beams, shorter counting times and improved statistical precision. Hence this article will review how these developments led to the widening of this field to a variety of samples, to data with higher experimental precision, and to studies involving a range of thermodynamic states.

The next section will cover (in general terms) the apparatus and methods used at the HASYLAB in Hamburg, the ESRF in Grenoble and the A.P.S. at A.N.L. in Chicago to measure the liquid structure factor $S(Q)$, where $\hbar Q$ is the momentum transferred in the scattering process. Then results on a variety of hydrogeneous and deuterated samples will be reviewed in subsequent sections. It will be evident that this field is now a reasonably developed one, which may be exploited (by scientists using these machines) for a variety of scientific purposes: including studies of hydrogen bonding effects, H–D isotopic difference effects, the relative structural importance of different hydrogeneous groups contained within intermolecular structures, and also for the improvement of the various methods used in these experiments.

2. EXPERIMENTAL METHODS

As discussed in Part I it has been advantageous to use high energy E.M. radiation in order to reduce the experimental corrections and improve the quality of the data as compared to normal X-ray work. With the advent of the machines listed in the previous paragraph, it has become possible to use high intensity beams of about 100 keV (E.M. radiation). Over the past few years this has allowed experiments of high precision, using relatively small samples, to be conducted in relatively short time periods (e.g. [2]). Also a variety of samples (made of H or D isotopes) have been studied using these instruments.

Figure 1 is a sketch illustrating a typical layout used for such experiments [2]. The incident beam is highly polarized (~90%) in the horizontal plane, and has a wavelength of (approximately) 0.11 Å. Consequently the scattering angles range over a few degrees only, which minimizes the standard X-ray corrections [3]. Also the high intensity available allows measurements of the scattered intensity as a function of the angle of scatter to be conducted in a few hours, even with small and thin samples. The reduction of the experimental data to molecular distribution functions has been described in a number of textbooks (e.g. [4]) and so will not be discussed here. Also the corrections to the experimental data which will reduce them to the structure factor $S(Q)$, may be found in the references cited and are listed also in Table 3 of Part 1.

The primary object of the research reviewed here has been to measure $S(Q)$ accurately in the cases of liquid or amorphous samples of simple molecular substances containing either H or D isotopes – e.g. water, benzene, alcohols etc. In the following sections a number of these experiments will be reviewed, and some interpretive comments will be presented. For the interpretation of the data it is assumed usually that

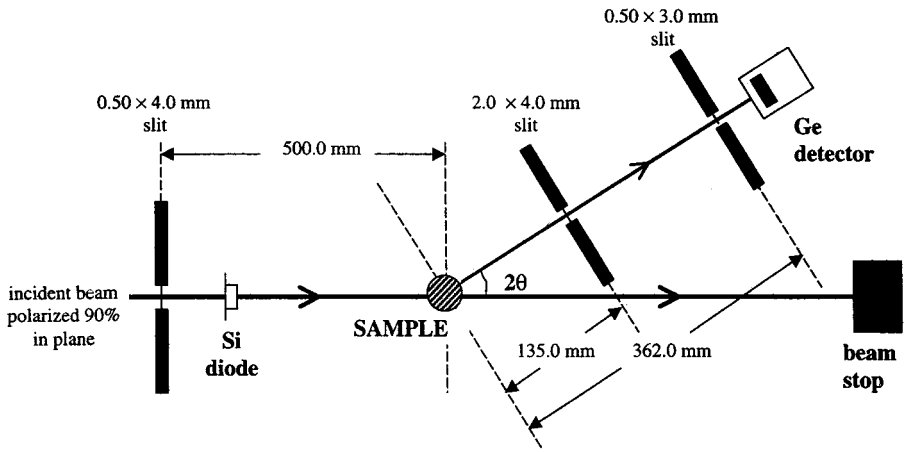

FIGURE 1 A schematic layout of the diffraction apparatus used at the ESRF [2].

the electron density in the isotopically different molecules (being compared) is indistinguishable, and this assumption has been checked experimentally for light and heavy water by Neuefeind *et al.* [5] and found to be satisfactory. The data will be presented here as pair correlation functions ($g_x(r)$ or $g(r)$) in either the X-ray form (denoted by the subscript x) or converted to the nuclear form and shown without the subscript.

3. WATER AND BENZENE – CONTRASTING HYDROGENEOUS LIQUIDS

Since water is a hydrogen bonded liquid at room temperature while benzene is not so bonded, they make an interesting pair of liquids to compare. How does the difference between the hydrogeneous and deuterated versions of the structure factors (for each of these liquids) compare in shape and magnitude? Recently synchrotron radiation scattering experiments, at room temperature, have been conducted on water by Tomberli *et al.* [2] and on benzene by Benmore *et al.* [6].

Figure 2 shows the pseudo internuclear pair correlation functions ($g(r)$) for benzene [7] and water [8] taken from the earlier literature. It is clear that their intermolecular structures differ considerably due to the local structure produced by the hydrogen bonding in water, which is absent in benzene. Thus one of the objects of these new experiments [2,6] was to compare the H–D liquid structure difference data (at room temperature) on these two liquids.

It would be useful to discover whether the new data exhibited similar effects to those shown by the pair correlation functions in Fig. 2. This figure shows a sharp intermolecular peak in water at 2.8 Å (due to H-bonding generating an ordered structure), and contrasts to a very broad peak in benzene (around 5 Å) due to the lack of an ordered structure. However the differences between the new D and H measurements on these two liquids [2,6], which are shown in Fig. 3 for the range 1–7 Å, cover both the intra- and inter-molecular regions. By comparing Figs. 2 and 3 it may be seen that the structural differences (shown in [2]) are carried into the inter-molecular differences seen in Fig. 3 in somewhat different ways. For water there are intermolecular peaks at 2.8 and 4.5 Å in both plots, while for benzene Fig. 3 shows a broad peak at 4.5 Å which

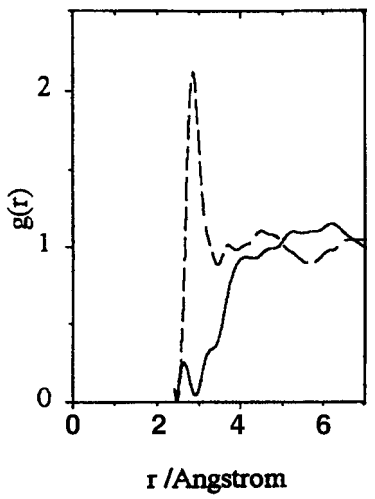

FIGURE 2 The pseudonuclear intermolecular correlation functions for water (dashed line) and benzene (full line) at room temperature, taken from early papers [7,8]. The region below 2.5 Å, which is omitted, would cover the structure of the molecules.

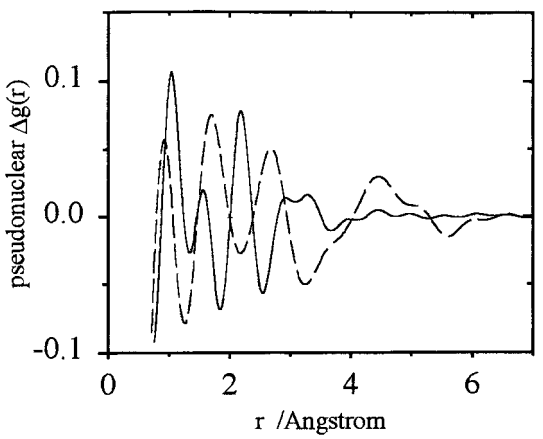

FIGURE 3 The difference, $\Delta g(r)$, in the intra plus inter total pseudonuclear correlation functions of water (dashed line [2]) and benzene (full line [6]) at 24°C and under their natural vapor pressures. These curves are for the deuterated sample minus the hydrogenated sample.

must correspond to a broadening or shift of the $r \sim 3$ to 6Å region in Fig. 2 for deuterated compared to hydrogenated benzene. Thus these isotopic structural differences are related to the underlying features of the intermolecular pair correlation functions.

However the intramolecular differences are the most striking ones in Fig. 3 – that is the structure at $r < 2.5$ Å – where the effect observed for benzene is relatively large. It was shown [6] that this may be explained by a slight broadening and shifting of the intra-molecular peaks in C_6H_6 compared to C_6D_6. In contrast this model did not work for water, and its peaks at $r = 0.93$ and 1.7 Å have been shown to be related to differences in the hydrogen bonding in light and heavy water [6]. These results have demonstrated the quality of the data that can be obtained using modern 100 keV

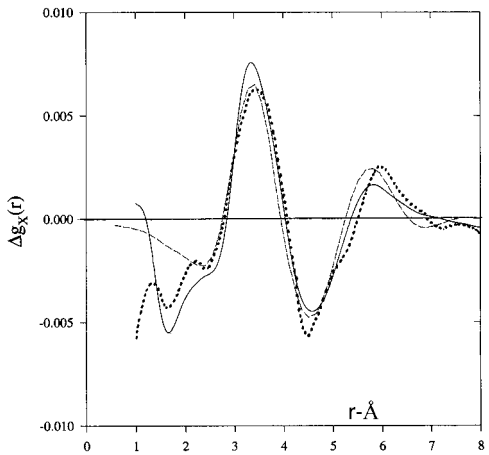

FIGURE 4 A comparison of the changes in $g_x(r)$ produced for water from the room temperature experimental isotopic changes ($H_2O - D_2O$) (full line [2]; dotted line [10]), and from a temperature change in light water of 5.5°C taken about 11.2°C (dashed line [9]).

sources, and they illustrate the information that may be obtained from detailed differences in the structure factors for H and D liquids composed of the same molecules.

An understanding of the magnitude of the observed effects in water may be obtained from a comparison between the $\Delta gx(r)$'s produced by changing isotopes to those observed by varying the temperature of one isotopic sample ([2], Fig. 9). This comparison is shown in Fig. 4, and temperature shift data were taken on either side of the density maximum in light water at 11.2°C [9]. The data from [2] are shown by the full line, while those from a more recent experiment by Badyal *et al.* [10] are shown by the dotted line. There is excellent agreement between these two experiments, which confirms that the present day techniques may yield high precision data. The dashed line shows the 5.5°C temperature shift data [9], and is in good agreement with the experimental results. Badyal *et al.* [10] also measured isochoric data and showed that they were consistent with the isothermal data – a very useful result. Therefore the similarity between the isotopic differences and the temperature differences suggests that a reasonable way to compare different isotopic samples of water is to choose appropriate temperature differences which equalize the underlying isotopic structures. A comparison of isotopic and temperature differences for a number of other samples would be worthwhile.

4. AMORPHOUS ICE

This topic was introduced in Part I (Section 4a) where early experiments [11] on the structures of amorphous ice samples were discussed. Differences, as a function of Q, between structure factor data on light and heavy amorphous ice at 77 K were shown at (Part I) Fig. 2b. However the preparation of the samples for experiments to measure these differences requires careful planning, since the (non-equilibrium) states being studied need to be related carefully. In the cases shown in Part I the samples were prepared at different times in different laboratories, and therefore their comparison

may yield only a first approximation to their differences. An interesting experiment would be to compare the isotopic difference observed for amorphous ice with that for liquid water. By comparing Figs. 2b and 3a of Part I it became clear that there was some similarity between these data for $Q < 4\,\text{Å}^{-1}$, which is the most important region. Consequently improved experiments allowing a better comparison would be worthwhile.

As a first step a summary of the several states of amorphous ice will be presented. Although two kinds of amorphous ice have been known and studied for a number of years [12], the full range of such states has been discovered only recently [13]. The H_2O ice was studied by the diffraction of E.M. radiation, and D_2O ice by thermal neutron diffraction. Figure 5(a) shows some results from the neutron diffraction experiments on D_2O ice conducted by Tulk *et al.* [13], in which they measured the position of the first diffraction peak in high density amorphous (HDA) as a function of time. It can be seen that this peak position varies with the length of the annealing time and becomes approximately constant after about 400 min annealing. But if the temperature is changed by 5 degrees the sample anneals to a new state, and seems possible that there could

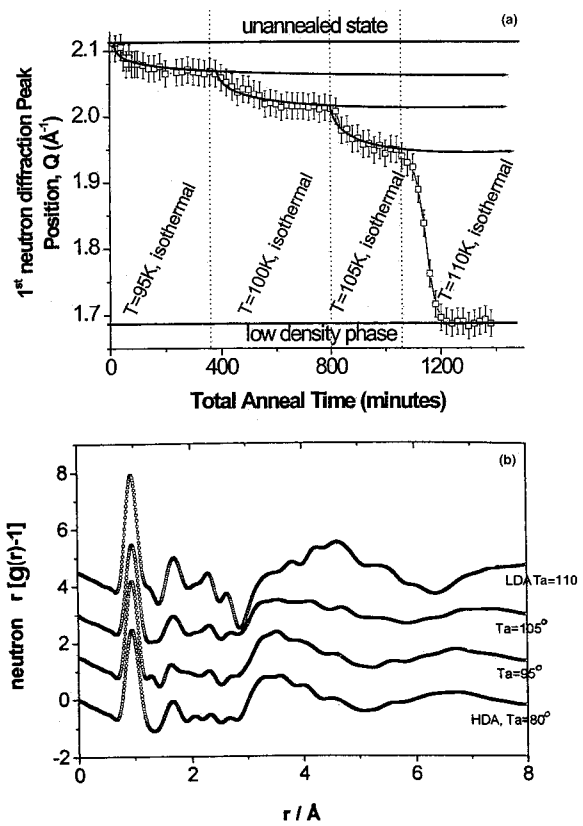

FIGURE 5 (a) The position of the 1st diffraction peak in the neutron structure factor ($S(Q)$) as function of the annealing time for an amorphous ice sample. The figure starts (at top left) with HDA ice and shows the steps the sample follows in moving to LDA ice [13]. (b) The pair distribution functions from the neutron diffraction experiments used for the data in Fig. 5a.

be many such states between HDA and low density amorphous (LDA). In this experiment after passing through four states and then annealing at 110 K the sample was observed to move to the well known LDA state. The structure factor data (from which Fig. 5(a) was derived) have been transformed [13] to the nuclear distribution functions. They are shown in Fig. 5(b) with those for HDA and LDA. It may be seen that as the temperature is changed from 80 to 110 K the intermolecular structure (from 3 to 8 Å) moves to somewhat larger values of r in an approximately smooth fashion. However these effects make the comparison of H with D amorphous ices somewhat complex, and therefore we shall compare the LDA ices only. There are a number of measurements in the literature, but we need data which allow accurate comparisons to be made.

At present detailed structural studies on LDA have been conducted by Urquidi *et al.* [14]. Using conventional methods they prepared samples of LDA ice, and subsequently cooled them to 40 K for diffraction experiments using synchrotron radiation at the Argonne Photon Source. Care was taken to follow similar procedures for both light and heavy water at all stages. The difference function between the D_2O and H_2O structure factors is shown at Fig. 6; where it may be compared to the difference in structure factors for a temperature shift of 8.9°C in H_2O LDA ice. It may be seen that the two curves are very similar. Also the shape of this difference curve is similar to that obtained for water at room temperature, for a similar temperature shift.

This conclusion that the isotopic difference between the light and heavy water structure factors is equivalent to a small temperature change (of about 9°C), even over a wide change in thermodynamic states, is worth further investigation. However it is a very useful result which may be employed in experiments whose object is to deduce partial structure factors from measured isotopic structure factor data. A recent experiment by Finney *et al.* [15] on partial structure factors of amorphous ice

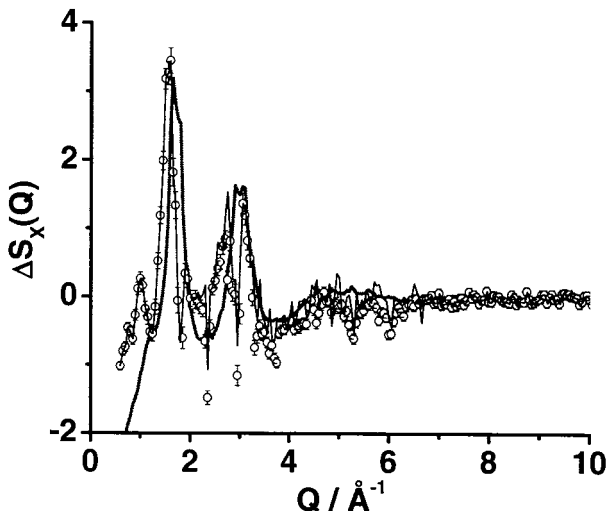

FIGURE 6 The difference $\Delta S_x(Q)$ in structure factors for E.M. radiation measured for LDA ice cooled to 40 K [14]. Circles (joined by the thin line) show the $D_2O - H_2O$ difference in $S_x(Q)$, and the heavy black line shows the temperature difference data for the H_2O sample (40 K data − 120 K data)/9 – equivalent to an 8.9 K shift.

at 80 K (measured by neutron diffraction) was analyzed without allowing for this effect. Thus it provides an example of an experiment which might employ this technique to improve the interpretation of the data.

5. METHYL ALCOHOL AT ROOM TEMPERATURE AND −80°C

In the cases of the molecules studied in Section 3 the sites for the H atoms in H_2O are equivalent, and also those within C_6H_6 are equivalent. This feature made the interpretation fairly straightforward. However in this section we look at a case where each molecule has more than one type of site - for example in CH_3OH there are two kinds of sites.

Synchrotron radiation scattering experiments were conducted on isotopic samples of liquid methanol, using instruments at DESY in Hamburg and ESRF in Grenoble, by Tomberli *et al.* [16]. Their experiments were performed using the methods described in Section 2 and the layout shown in Fig. 1. The samples studied included, CH_3OH, CD_3OD, CH_3OD, CD_3OH, and comparisons between them were published in both the experimental Q-space and in real r-space after Fourier transformations. Here we will discuss their data using the r-space transformations.

Figure 7(a) shows the simplest comparison, namely the methanol $\Delta g(r)$ difference between measurements made at 23.5°C on samples of CH_3OD and CH_3OH. The largest peak occurs at 1.4 Å, which is the position of the leading peak in $g(r)$ corresponding to the (intra) C–O distance. However its amplitude is approximately 2% of the peak height observed in $g(r)-1$. The next peak occurs at $r \simeq 2$ Å where there is a valley in $g(r)$, and the peak at $r = 2.5$ Å does not correspond to any feature in $g(r)$. The calculated (using the IAA) intramolecular difference is shown by the dashed line and its shape is similar to the observed effect for $r < 1.7$ Å. In Fig. 7(b) we show the difference in the structures of liquids CD_3OH and CH_3OH at 23.5°C, compared to intramolecular difference shown by the dashed line. It may be seen that there is overall similarity near 1 Å (in contrast to Fig. 7(a)), but differences are observed as expected at higher r. Differences between data [16] on [CD_3OD–CH_3OH] and the results in Fig. 7 are outside the estimated experimental errors, and so may be used to put a limit on the accuracy of published partial pair functions derived from neutron scattering results on these samples.

Tomberli *et al.* [17] compared these effects in liquid methanol at room temperature and with those at −80°C, and their results (between 1 and 5 Å) for the several differences are shown in Fig. 8. The methyl difference (shown by the dashed line) is the largest effect for $r > 1.5$ Å, and a computer simulation of the difference between the dashed (methyl effect) and solid (hydroxyl effect) lines would be helpful. The room temperature methyl effect (shown by the dash–dot line) is comparable to the low temperature hydroxyl effect for $r > 2$ Å and is comparable to the methyl effect at $r \sim 1.4$ Å. Detailed computer simulations of the structures of these liquids would throw light on the reasons for such effects.

Finally Benmore *et al.* [18] discuss the improvement that may be obtained in neutron diffraction data (at −30°C) by operating a CD_3OH sample at 5.5°C warmer than the CD_3OD sample. Figure 9 compares the change in these two X-ray $S(Q)$'s – $\Delta S_x(Q)$ – obtained by direct measurements on both samples, with the change produced by the temperature shift of 5.5°C on the CD_3OD sample. The satisfactory agreement has

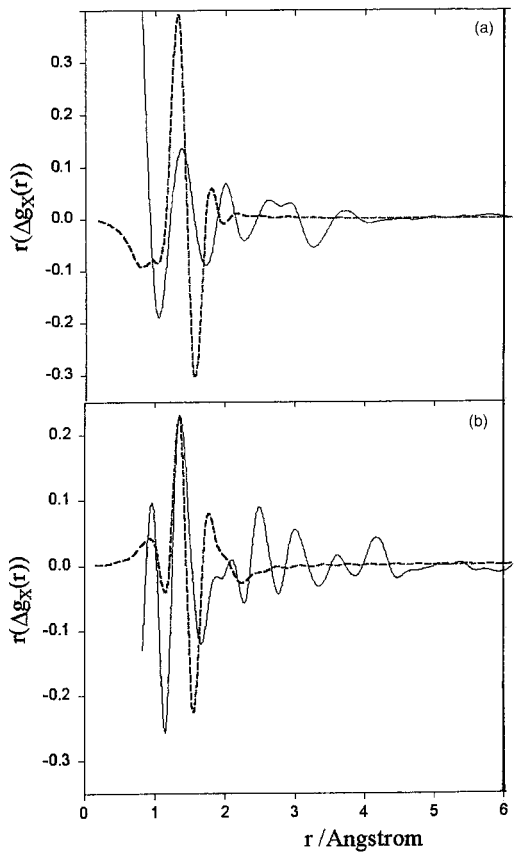

FIGURE 7 (a) The isotopic difference in pair correlation functions ($\Delta g_x(r)$) for the molecular liquids (CH_3OD–CH_3OH) at 23.5°C (full line), and the calculated intramolecular isotopic difference (dashed line) [16]. Note the differences between 7(a) and (b) over the whole range of r. (b) The isotopic difference in pair correlation functions ($\Delta g_x(r)$) for the molecular liquids (CD_3OH–CH_3OH) at 23.5°C (full line), and the calculated intramolecular isotopic difference (dashed line) [16]. These data, (a) and (b), are plotted as $r\,\Delta g$ to enhance the larger r effects.

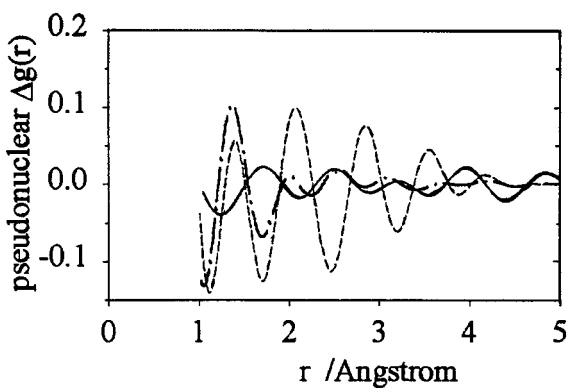

FIGURE 8 The isotopic difference in pair correlation functions ($\Delta g(r)$) for the molecular liquids (CD_3OH–CH_3OH) at −80°C (dashed line) and (CD_3OD–CD_3OH) at −80°C (solid line) [17]. They may be compared to room temperature (dash–dot line) for the difference (CD_3OH–CH_3OH) at 24.5°C.

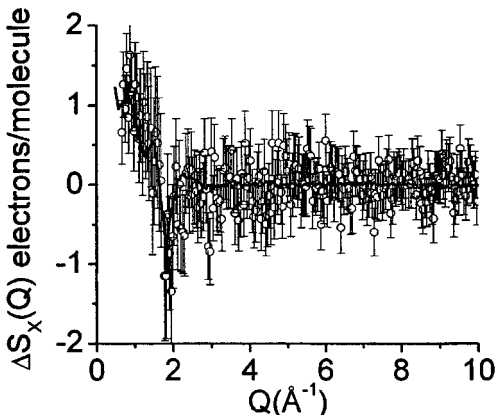

FIGURE 9 The difference in the electronic structure factors $\Delta S_x(Q)$ for the molecular liquids (CD_3OD–CD_3OH) [circles with errors] compared to the temperature derivative for CD_3OD [$(S_x(25°C)–S_x(-30°C))/10$] shown by the line [18].

allowed this technique to be employed in neutron diffraction experiments. Of course each pair of samples used in the neutron experiments needs to be evaluated in this way. Finally it is interesting to observe that this temperature shift has the same magnitude as that observed for water and discussed in connection with Fig. 4. A listing of all the observed methanol differences is given in the Appendix.

6. ETHYL ALCOHOL

Molecules of ethyl alcohol (CH_3CH_2OH) contain three molecular groups, and therefore their structures and motions are more complex than the cases considered above. Moreover there are twelve varieties of these molecules which contain different combinations of the H and D atoms (if CH_3 and CH_2 are treated as units). In the work described by Tomberli *et al*. [19] five different molecular liquids (giving four differences) were measured. They used the techniques discussed in Sections 1 and 2, and the set of four differences they observed are shown in Fig. 10. It is perhaps striking that the topmost line in this figure (methyl substitution) produces the smallest amplitude. However, if the upper three curves (each involving a single substitution) are added together (and the total halved), they form a good match to the effect obtained by subtracting the fully hydrogenated data from the fully deuterated data (bottom figure). Theoretical investigations and computer simulations would be useful in order to understand the data in Fig. 10 in more detail. And, of course, the extension of these data to additional examples of H–D combinations in ethanol molecules, will lead to deeper insight into the behavior of such complex molecules.

7. CONCLUSIONS

The examples quoted here of experiments involving the measurement of differences in the radial distribution functions (using data on structure factors) of hydrogeneous compared to deuterated liquids and glasses, have shown how this field has matured.

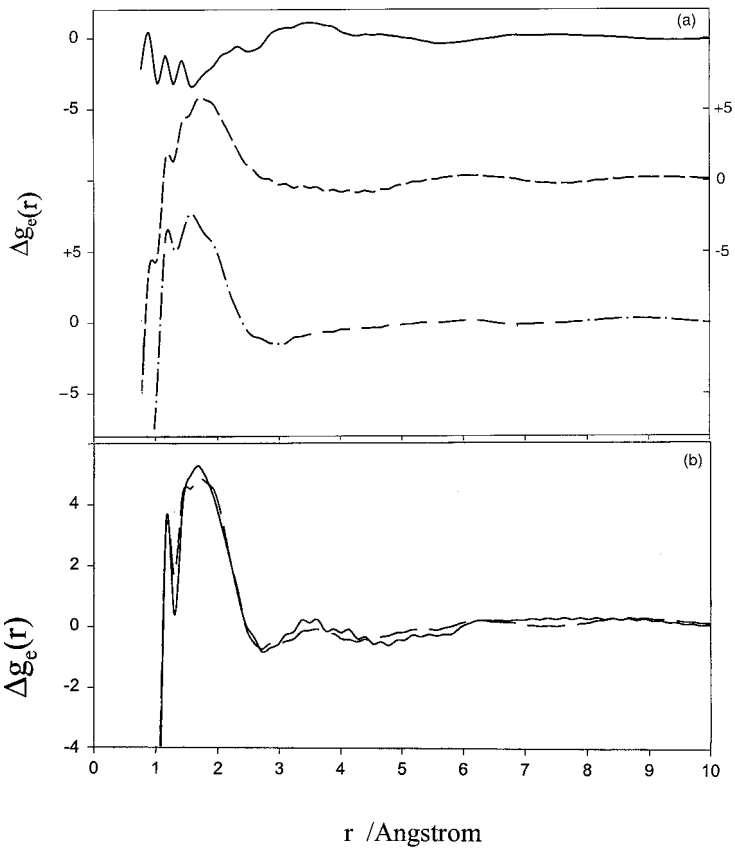

FIGURE 10 The isotopic difference in electronic pair correlation functions, $\Delta gx(r)$, for liquid ethanol [19]: (a) full line (CD_3CH_2OH–CH_3CH_2OH), dashed line (CH_3CD_2OH–CH_3CH_2OH), dashed–dot line (CH_3CH_2OD–CH_3CH_2OH); (b) full line (CD_3CD_2OD–CH_3CH_2OH), dashed line – the sum of the three functions in Part (a) divided by 2.

Now these differences can be studied (in fairly routine ways) once suitable samples have been prepared, and this has led to deeper insights into several structural problems, as shown in Figs. 2–11. Perhaps the most striking result has been that the same temperature shift has been found to be equivalent to the structural isotopic effect in the case of two different samples (water and methanol) and of same magnitude in amorphous ice. Obviously this effect may be exploited by experimentalists doing partial structure factor experiments. However it should be investigated theoretically as well which may lead to further interesting results.

With future developments (especially in the variety of samples) one may expect many more interesting results, which will lead to the wider use of these data. The applications of these results to fields of science other than structural problems is speculative at present, but one may anticipate that the interesting scientific information presented here will find a variety of uses in these areas. One example would be the application to medical, chemical, or biological problems where isotopic effects are being studied or may be involved.

Acknowledgment

I wish to thank my colleagues Bruno Tomberli, Jörg Neuefeind and Chris Benmore for many helpful discussions on the topics reviewed in this paper.

References

[1] P.A. Egelstaff (1983). In: I. Prigogine and S.A. Rice (Eds.), *Advances in Chemical Physics*, Vol. LIII, p. 1. John Wiley and Sons, N.Y.
[2] B. Tomberli, C.J. Benmore, P.A. Egelstaff, J. Neuefeind and V. Honikimäki (2000). *Phys. Condens. Matt.*, **12**, 2597
[3] H.H. Paalman and C.J. Pings (1963). *Rev. Mod. Phys.*, **35**, 389.
[4] P.A. Egelstaff (1994). *An Introduction to the Liquid State*, Ch. 3. Clarendon Press, Oxford.
[5] J. Neuefeind, C.J. Benmore, B. Tomberli and P.A. Egelstaff (2002). *J. Phys. Condens. Matt.*, **14**, L429.
[6] C.J. Benmore, B. Tomberli, P.A. Egelstaff and J. Neuefeind (2001). *Molecular Phys.*, **99**, 787.
[7] A.H. Narten (1977). *J. Chem. Phys.*, **66**, 3117.
[8] A.H. Narten and H.A. Levy (1971). *J. Chem. Phys.*, **55**, 2263.
[9] L. Bosio, S. Chen and J. Teixeira (1983). *Phys. Rev. Lett.*, **A27**, 1468.
[10] Y.S. Badyal, D.L. Price, M.L. Saboungi, D.R. Haeffner and S.D. Shastri (2002). *J. Chem. Phys.*, **116**, 10833.
[11] A. Bizid, L. Bosio, A. Defrain and M. Oumezzine (1987). *J. Chem. Phys.*, **87**, 2225.
[12] O. Mishima, L.D. Calvert and E. Whalley (1984). *Nature*, **310**, 393
[13] C.A. Tulk, C.J. Benmore, J. Urquidi, D.D. Klug, J. Neuefeind, B. Tomberli and P.A. Egelstaff (2002). *Science*, **297**, 1320.
[14] J. Urquidi, C.J. Benmore, J. Neuefeind, B. Tomberli, C.A. Tulk, P.A. Egelstaff and D.D. Klug (2003). *Journal of Physics. C.*
[15] J.L. Finney, A. Hallbrucker, I. Kohn, A.K. Soper and D.T. Brown (2002). *Phys. Rev. Letts.*, **88**, 22503.
[16] B. Tomberli, P.A. Egelstaff, C.J. Benmore and J. Neuefeind (2001). *J. Phys. Condens. Matt.*, **13**, 11405 (Part 1) and 11421 (Part 2)
[17] B. Tomberli, C.J. Benmore, P.A. Egelstaff, J. Neuefeind and V. Honkimäki (2401). *Europhysics Letters*, **55**, 341.
[18] C.J. Benmore, B. Tomberli, J. Neuefeind and P.A. Egelstaff (2002). *Applied Physics*, **A75**, 1.
[19] B. Tomberli, C.J. Benmore, J. Neuefeind and P.A. Egelstaff (2002). *Can. J. Phys.*, **80**, 1059.

APPENDIX

A Summary of Methanol Differences in *r* space

In designing experiments involving the structures of hydrogeneous and deuterated molecules it is useful to have a summary of the type of data covered in this review. As an example the methanol data (at room temperature) reviewed at Section 5 will be presented in this form.

Since the major effect occurs over the range $0.9 < r < 2.6\,\text{Å}$ these examples will be restricted to that range only. Figure 11 presents six diagrams covering all possible cases for this molecule (when CH_3 is treated as a unit). The height of the C–O peak at 1.4 Å is approximately 1.5 in the function $g(r) - 1$, which may be compared to an average of ~0.15 for these $\Delta g(r)$ data. In Fig. 11 the differences have been selected so that this peak is positive in the difference functions. Therefore the first member of each pair has the sharper C–O peak. Also there are significant differences between these diagrams, both in their magnitude and in the nature of the molecular group which produces the major effect? Therefore in addition to their use in improving partial structure factor results, they will be useful in testing molecular interaction models as well.

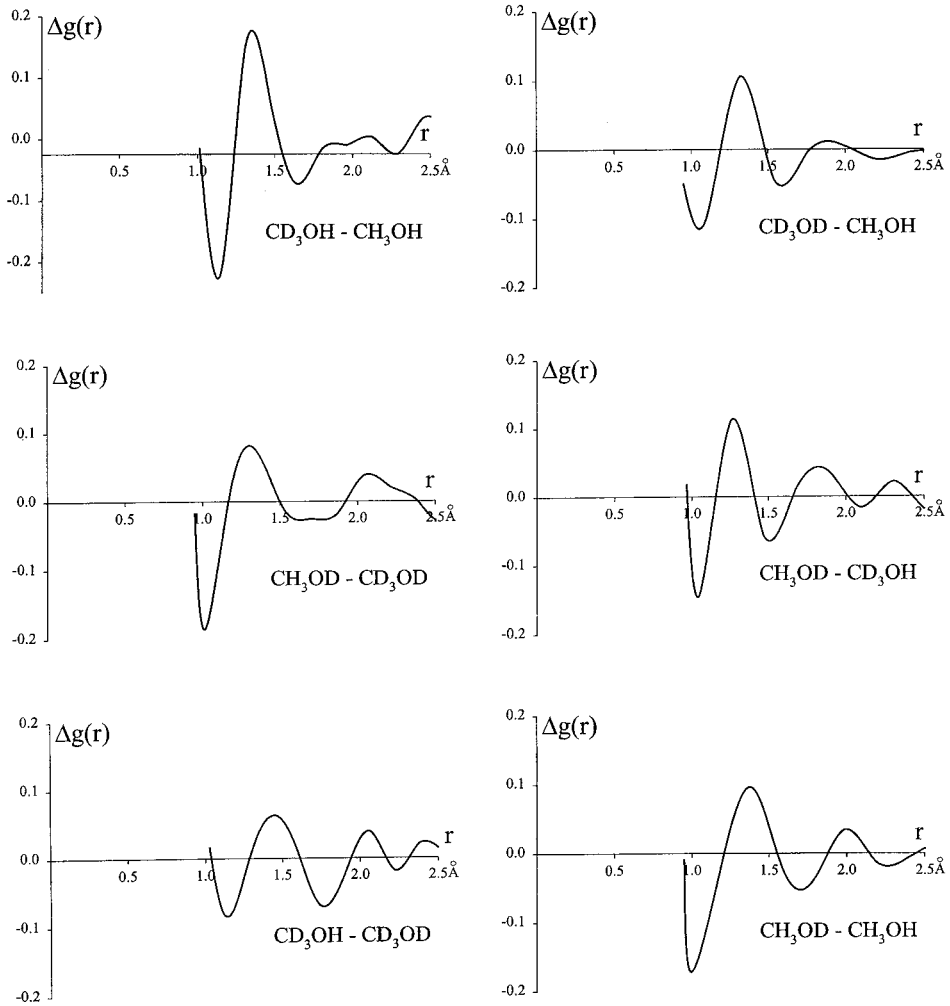

FIGURE 11 A summary figure showing the six measured [16] differences in $g(r)$ for methanol isotopic liquids over the Q-range of greatest intensity.